Hindawi Publishing Corporation
Journal of Materials
Volume 2014, Article ID 184340, 8 pages
http://dx.doi.org/10.1155/2014/184340

Research Article

Preparation, and Structural and Magnetic Properties of Ca Substituted Magnesium Ferrite with Composition $MgCa_xFe_{2-x}O_4$ ($x = 0.00, 0.01, 0.03, 0.05, 0.07$)

K. K. Bamzai,[1] Gurbinder Kour,[1] Balwinder Kaur,[1] and S. D. Kulkarni[2]

[1] *Crystal Growth & Materials Research Laboratory, Department of Physics and Electronics, University of Jammu, Jammu 180006, India*
[2] *National Chemical Laboratory, Homi Bhabha Road, Pashan, Pune 411008, India*

Correspondence should be addressed to K. K. Bamzai; kkbamz@yahoo.com

Received 10 December 2013; Revised 24 March 2014; Accepted 29 March 2014; Published 22 April 2014

Academic Editor: Christian M. Julien

Calcium substituted magnesium ferrite with composition $MgCa_xFe_{2-x}O_4$ (where $x = 0.00, 0.01, 0.03, 0.05, 0.07$) was prepared by ceramic technique. These compositions were then subjected to detailed study for structural and magnetic properties. X-ray diffraction studies reveal the formation of single phase cubic spinel. The values of lattice constant increase with the increase in calcium concentration from $x = 0.00$ to $x = 0.03$ and then decrease. Scanning electron microscopic (SEM) technique was used to study the morphology of the grown materials. The grain size was calculated using average intercept line method. The elemental composition of pure and calcium substituted magnesium ferrite was obtained from energy dispersive X-ray analysis (EDAX) spectrum. The hysteresis loop confirms the magnetic behaviour of the prepared composition, which is then discussed on the basis of cation distribution. The parameters such as saturation magnetization, coericivity, and retentivity are calculated. The Curie temperature was found to decrease with increasing calcium content.

1. Introduction

Magnesium ferrite has attracted attention as one of the ferrites for high density magnetic recording, microwave absorbents, sensors and electronic device, high frequency devices, colour imaging, and so forth, because it has high magnetic permeability and high electrical resistance [1–4]. $MgFe_2O_4$ is a partially inverse spinel [5, 6] and can be considered as a collinear ferrimagnet whose degree of inversion is sensitive to the sample preparation history. Magnesium ferrite with diamagnetic substitution for Mg^{2+} and Fe^{3+} ions has attracted the attention of a number of research workers who attempted to explain the magnetic properties on the basis of the distribution of the only magnetic ion Fe^{3+} in tetrahedral (A) and octahedral (B) sites, which makes the analysis reliable [7]. The physical and chemical properties of $MgFe_2O_4$ depend upon the cation distribution, which in turn is a complex function of processing parameters and method of preparation of the material [8]. The variation that is brought about in the physicochemical and electromagnetic properties due to a change in the particle dimension has encouraged many researchers around the globe to prepare spinel ferrites with novel properties.

The structural and magnetic characteristics of $MgFe_2O_4$ with nonmagnetic substitution such as Zn^{2+} [9], Cd^{2+} [10], Ti^{4+} [11], and Al^{3+} [12] have been investigated by means of X-ray diffraction (XRD) and magnetic measurement technique. Some work on various properties of spinel ferrites with Ca^{2+} substitution such as $CoFe_2O_4$ [13], Li-Zn ferrite [14], Cu-Zn ferrite [15], Ni-Zn ferrite [16], and $MgFe_2O_4$ [7] has also been reported.

Generally, Mg^{2+} and Fe^{3+} cations are distributed at both sites. The Fe_A^{3+}-Fe_B^{3+} super exchange interaction is normally different from the Mg_A^{2+}-Fe_B^{3+} interaction, so the variation of cation distribution over A and B sites in the spinel leads to different magnetic properties of these oxides even though the chemical composition of the compound does not change

[17]. Thus, determination of cation distribution between the tetrahedral and octahedral sites has been a subject of many studies [18–21]. Wei et al. [18] from the X-ray diffraction studies proposes that, with manganese ion substitution, Mn^{3+} ions predominately occupy the octahedral site, whereas Fe^{3+} ion decreases linearly, thereby suggesting that Fe^{3+} is being replaced by Mn^{3+} ion on substitution.

In the present paper, calcium (Ca) substituted magnesium ferrite is reported with a view to study the effect of substitution of nonmagnetic ion (Ca^{2+}) on the structural and magnetic behaviour. The free ionic radius of the cations involved is Mg^{2+} (0.66 Å), Ca^{2+} (0.99 Å), and Fe^{3+} (0.64 Å). Therefore, it would be interesting to substitute large cation Ca^{2+} (whose radius is near the threshold ~1 Å) for Fe^{3+} in $MgFe_2O_4$.

2. Materials and Methods

2.1. Materials Preparation. Pure magnesium ferrite (MgFe) and calcium substituted magnesium ferrite (CaMgFe) with composition $MgCa_xFe_{2-x}O_4$ (x = 0.00, 0.01, 0.03, 0.05, 0.07) were prepared using the ceramic technique. High purity oxides, 99.99% of CaO, MgO, and Fe_2O_3, were used as starting materials. The oxides of metal ions were mixed together according to their molecular weight. The mixture of each sample was ground to a very fine powder in agate mortar. The mixed powder was then transferred to electric ball mill for 48 hours. The dried powder was pressed into pellets and presintered at a temperature of 800°C for 2 hours with a heating rate of 2°C/min so that the initial chemical reaction between the constituents can take place. The presintered mixture was ground again and pressed into the required shapes using hydraulic press under a pressure of 120 kg/cm^2 in order to obtain a high degree of compaction. In the final sintering process, the samples were placed in a furnace heated up to 1200°C with a heating rate of 4°C/min, kept for 2 hours, and then cooled to 900°C at the rate of 7.5°C/min after which it was cooled to room temperature. After sintering, the compacts were polished to remove the surface layers to ensure that the measured properties correspond to those of the bulk and not the surface layers.

2.2. Characterization. In order to confirm the completion of solid state reaction as well as analyzing the crystalline phase and the structural parameters, X-ray diffraction patterns of the powdered samples were recorded by using a Rigaku powder X-ray diffractometer using Cuk_α (λ = 1.54059 Å) radiation. The shape, size, and distribution of pure and calcium substituted magnesium ferrite were carried out with the help of scanning electron microscope (SEM Model LEO 440 PC Based DIGITAL SEM). The elemental composition was confirmed with the help of energy dispersive X-ray analysis (EDAX model OXFORD: LINK ISIS, 300). A fully computer controlled vibrating sample magnetometer (VSM: EG&G Princeton, Applied Research Model 4500) was used for magnetization (with a maximum applied field of 15 kOer at room temperature) and Curie temperature measurements.

Table 1: Variation of grain size with different composition of Ca, that is, $MgCa_xFe_{2-x}O_4$ (where x = 0.00, 0.01, 0.03, 0.05, 0.07).

Composition	Size (μm)
Pure MgF	3.99
Ca 1%	3.26
Ca 3%	2.37
Ca 5%	1.67
Ca 7%	1.30

3. Results and Discussion

3.1. Structural Properties. Figures 1(a)–1(e) show typical scanning electron microscopic (SEM) images of $MgCa_xFe_{2-x}O_4$ (where x = 0.00, 0.01, 0.03, 0.05, 0.07), respectively. It is clear from these electron micrographs that the material essentially consists of some irregularly cubic particles in pure Mg-ferrite (Figure 1(a)) and agglomeration of these particles increases with the increase in Ca^{2+} ions concentration. The grain size was calculated using the average intercept line (AIL) method [22]. Well-crystallized dense grains of irregular shapes were observed for these compositions with the presence of large micropores. The grain size of MgFe is 3.99 μm which decreases with increase in substitution. The continuous decrease in grain size with Ca substitution may be due to the fact that Ca^{2+} ions (0.99 Å) have large ionic radii than that of Fe^{3+} (0.64 Å) and, therefore, show limited solubility in spinel lattice and prevent grain growth resulting in decrease in grain size [23]. Table 1 shows the values of grain size with Ca^{2+} composition in Mg-ferrite.

Figures 2(a) and 2(b) show the energy dispersive X-ray analysis (EDAX) spectrum for 1 and 7% Ca substituted magnesium ferrite, whereas Table 2 gives quantitative estimation of elements obtained directly from spectrum through its atomic and weight percentages. The results confirmed the presence of the required elements in the prepared composition with almost all the peaks associated with elements such as those of Mg, Fe, O, and Ca, thereby suggesting the formation of pure MgFe and CaMgFe.

The X-ray diffraction (XRD) studies confirm the formation of polycrystalline cubic spinel phase. Figure 3 shows X-ray diffraction pattern indicating (hkl) values for pure and Ca substituted magnesium ferrite. The diffraction peaks corresponding to planes (220), (311), (400), (422), (511), and (440) provide a clear evidence for the formation of spinel structure of the ferrite [24]. The "d" values and intensities of the observed diffraction peaks match the crystalline cubic spinel form of the magnesium ferrite (JCPDS Card no: 36-0398).

The data on lattice parameter "a," X-ray density "D_x," bulk density "D_B," and porosity "P" is summarized in Table 3. The plot of lattice constant "a" (Å) versus calcium content (x) is depicted in Figure 4. It is found from the figure that lattice constant initially increases up to x = 0.03 and thereafter it decreases with further increase in "x." This indicates that the variation of "a" with "x" does not obey Vegard's law [25]. This nonlinear behaviour of "a" with "x" may be

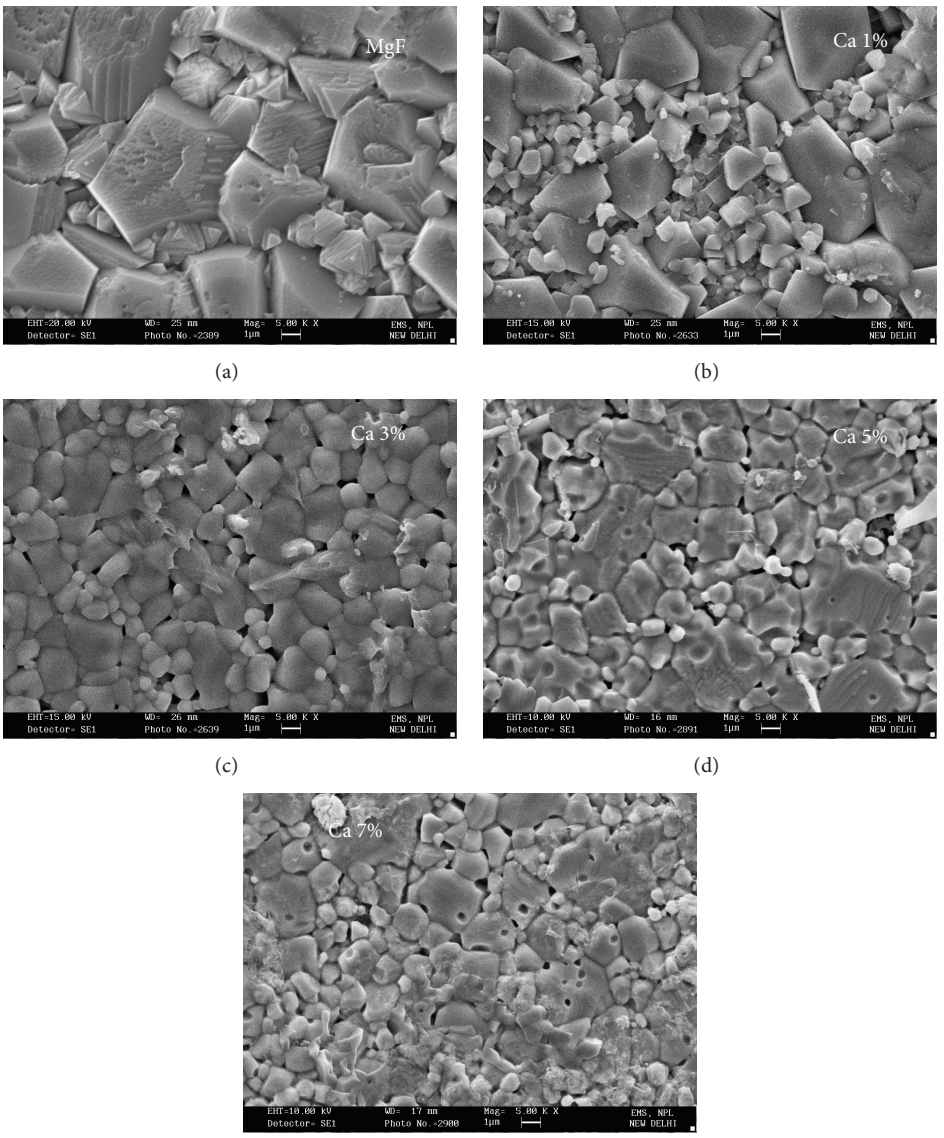

Figure 1: Scanning electron microscopic (SEM) photographs showing (a) pure $MgFe_2O_4$(MgFe), (b) 1% Ca substituted MgFe, (c) 3% Ca substituted MgFe, (d) 5% Ca substituted MgFe, and (e) 7% Ca substituted MgFe. The agglomeration of particles increases with increase in Ca concentration.

due to the substitutional effect of larger Ca^{2+} ions (0.99 Å) in magnesium ferrite. Further, nonlinear behaviour of "a" with "x" on the other hand is reported for the systems which are not completely normal or inverse [26]. The Ca^{2+} ions have strong preference for tetrahedral (A) site [27]. The Ca^{2+} ions, having the larger ionic radius (0.99 Å), when substituted in Mg-ferrite replace the smaller Fe^{3+} (0.64 Å) ions on the tetrahedral (A) sites; this causes linear rise in the lattice constant with "x" following Vegard's law for $x \leq 0.03$ and the maximum value of "a" is observed for this composition ($x = 0.03$). The decrease in the lattice constant at $x \geq 0.03$ can be attributed to the reduction of Ca^{2+} ions on the A-sites. The continuous decrease of lattice constant till $x = 0.07$ suggests that there is continuous reduction of Ca^{2+} ions on the A-sites of the cubic lattice. The deviation from the straight line thus also indicates incomplete Ca substitution in face centered cubic (fcc) phase. It is also reported in the literature that when doping percentage of Ca^{2+} ions is increased beyond 0.05%, the value of lattice parameter again decreases slightly. This is probably due to the fact that, for higher concentration, the Ca^{2+} ions occupy interstitial sites [20, 28].

The X-ray density (D_x) was calculated using the relation [29]

$$D_x = \frac{8M}{Na^3}, \tag{1}$$

where "M", "N," and "a" are the molecular weight, Avogadro's number, and lattice parameter, respectively. It is evident from

Table 2: Experimental values obtained from the spectrum of energy dispersive X-ray analysis for various constituent elements present in magnesium ferrite and calcium substituted magnesium ferrite.

Element	MgFe (pure)		MgFe (Ca 1%)		MgFe (Ca 3%)		MgFe (Ca 5%)		MgFe (Ca 7%)	
	At%	Wt%	At%	Wt%	At%	Wt%	At%	Wt%	At%	Wt%
O	57.65	31.49	58.39	31.94	60.13	34.33	56.43	31.35	56.66	33.11
Mg	10.93	9.07	10.16	8.44	10.09	9.03	11.54	9.74	13.77	12.23
Fe	30.93	58.98	30.62	58.47	25.0	49.82	26.20	50.80	19.73	40.25
Ca	—	—	0.84	1.15	4.77	6.82	5.83	8.12	9.84	14.41

Table 3: Lattice parameter "a," X-ray density "D_x," bulk density "D_B," and porosity "P" for different composition.

Composition	Lattice parameter "a" (Å)	X-ray density "D_x" (gm/cm^3)	Bulk density "D_B" (gm/cm^3)	Porosity "P" (%)
MgF (Pure)	8.3848	4.5062	3.864	15
Ca 1%	8.4108	4.4610	3.598	19
Ca 3%	8.4405	4.4071	3.225	26
Ca 5%	8.4211	4.4783	3.692	17
Ca 7%	8.4046	4.4721	4.061	9

Table 4: The values of saturation magnetization (M_s), coercivity (H_c), residual magnetization (M_r), and Curie temperature (T_C) for pure and substituted MgF.

Number of Ca atoms substituted	Saturation magnetization "M_s" (emu/g)	Coercivity "H_c" (Oer)	Residual magnetization "M_r" (emu/g)	Curie temperature "T_C" (°C)
0.00	23.5	26	1.52	400
0.01	22.5	28	1.53	388
0.03	24.5	31	2.00	370
0.05	30.7	20.5	1.38	331
0.07	29.0	30	1.96	325

the table that X-ray density decreases up to $x = 0.03$ and then increases which is attributed to the variation of "a" with "x" [30]. The change in density is divided into two regions. In the first region for the composition $x = 0.00$ to 0.03, there is decrease in the density, whereas, in the second region, the density increases. This behaviour starting from $x = 0.03$ to 0.07 [31] cannot only be ascribed to the replacement process between the lighter atom of Fe by the heavier atom of Ca but also be according to the distribution of Ca content among the sublattice and consequently the effect of condensation on the crystal structure. By comparing the bulk density and X-ray density, porosity of each composition can also be calculated.

The percentage porosity of the samples is calculated using the relation [32]

$$P\% = 1 - \frac{D_B}{D_x}, \tag{2}$$

where "D_B" and "D_x" are the bulk and X-ray density, respectively.

3.2. Magnetic Properties. It is well known that calcium ions can enter the spinel lattice up to a certain proportion [21], and its solubility limit is determined by the following three factors: (i) relatively larger ionic radius of Ca^{2+} ion [23] (as compared to the dimensions of A-tetrahedral or B-octahedral sites), (ii) the lattice constant of the spinel substituted by Ca, and (iii) the cooling rate of the ferrite after sintering [21, 33, 34]. Therefore, it is necessary to understand from their magnetic properties the behaviour of calcium substitution on the spinel lattice of MgFe.

Figure 5 displays the room temperature hysteresis loops for pure and Ca substituted MgFe, which indicates the soft ferrimagnetic nature of the synthesized particles. The values of the saturation magnetization (σ_s), coercivity (H_c), and retentivity (σ_R) can be obtained from this curve. It is clear from the figure that all the materials show a similar behaviour; that is, the value of magnetization increases with the increase in the value of applied field and gets saturated at a very low value of applied field approximately equal to 1000 Oer. From these hysteresis loops, one can obtain the information about the saturation magnetization (σ_s) and the same is given in Table 4. The interesting observation is that the value of saturation magnetization is maximum in the sample for Ca5% substitution and minimum for Ca1% substituted MgFe.

The value of saturation magnetization in pure $MgFe_2O_4$ is 23.5 emu/gm which decreases to 22.5 emu/gm for Ca1% and then starts to increase with 24.5 emu/gm for Ca3% and

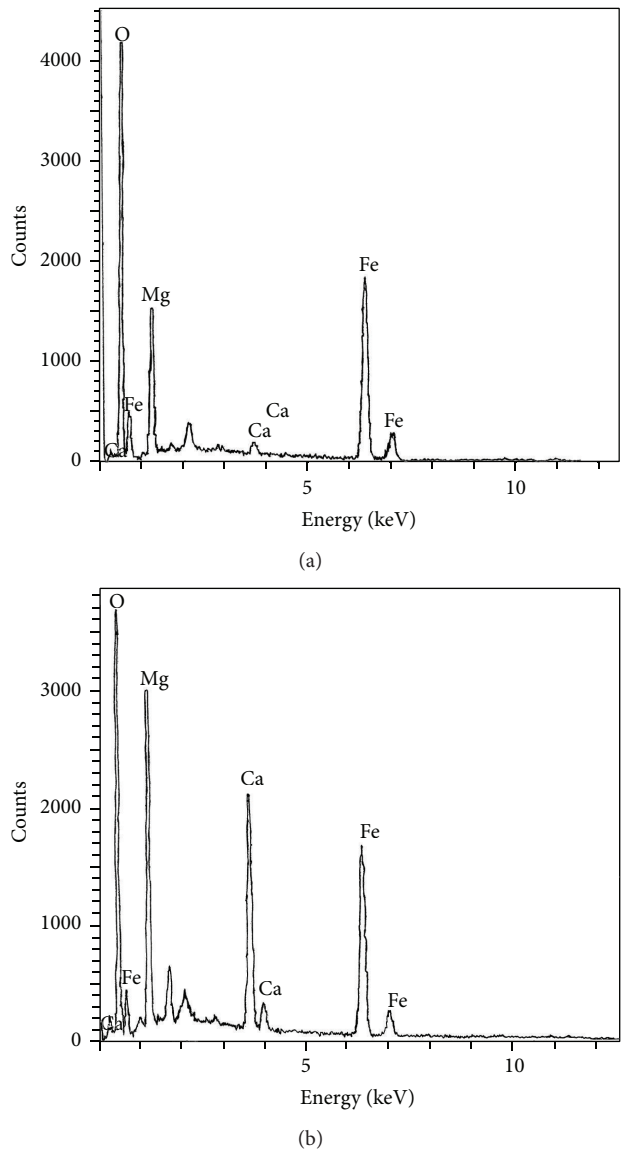

Figure 2: Energy dispersive X-ray analysis (EDAX) spectrum for (a) 1% Ca substituted and (b) 7% Ca substituted MgFe showing all the constituent elements expected to be present in the prepared material.

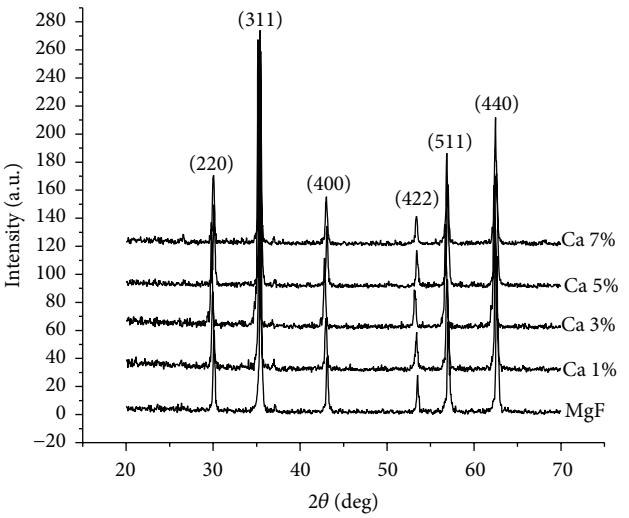

Figure 3: X-ray diffraction pattern of pure and Ca^{2+} substituted $MgFe_2O_4$ representing the formation of polycrystalline cubic spinel phase.

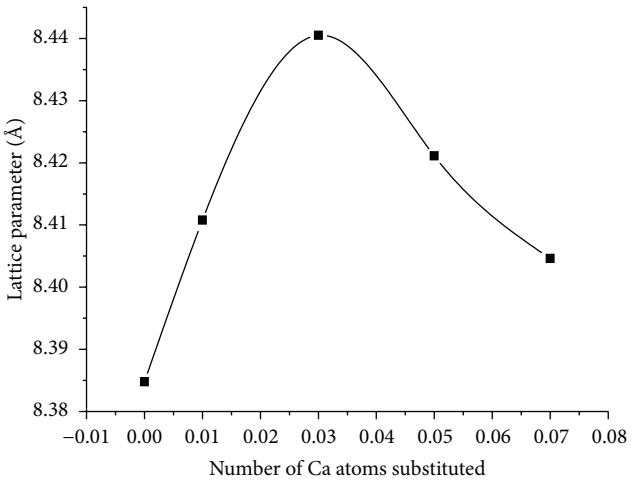

Figure 4: Variation of lattice parameter "a" of the composition $MgCa_xFe_{2-x}O_4$ (x = 0.0, 0.01, 0.03, 0.05, 0.07) as a function of concentration "x".

30.7 emu/gm for Ca5%, followed by further decrease with 29.0 emu/gm for Ca7% substituted magnesium ferrite. Smit and Wijn [35] have reported saturation magnetization value for bulk particles of $MgFe_2O_4$ as 27 emu/gm, whereas, in the present case, the value comes out to be 23.5 emu/gm. The difference in the value of saturation magnetization can be explained in the light of cation distribution. Any change in the concentration and nature of ions in A- and B-site causes resultant magnetization to be different from the reported one [1].

The composition dependence of magnetization can be explained on the basis of cation distribution. It is reported [35] that the metal ion distribution in $MgFe_2O_4$ is given by

$$\left(Mg_{0.1}Fe_{0.9}\right)_A\left[Mg_{0.9}Fe_{1.1}\right]_B \quad (3)$$

The case of Mg-ferrite is somewhat exceptional. Its structure was originally reported to be inverted, that is, having the same number of magnetic atoms on A-sites as on B-sites [36]. On the basis of the Neel coupling scheme, Mg-ferrite would then be expected to have zero saturation moment. However, this was not observed experimentally and the saturation moment was found to vary within the limits of 1–2.4 Bohr magnetons depending on the conditions of preparation [37]. This discrepancy has been explained on the assumption that Mg-ferrite is incompletely inverted; the number of iron atoms on B-sites thus exceeds the number on A-sites. Smit and Wijn [35] reported the magnetic moment per molecule $MgFe_2O_4$ at 0 K as 1.1 Bohr magnetons.

In the present system, the magnetic properties are sensitive to the distribution of Fe^{3+} ion in A- and B-sites.

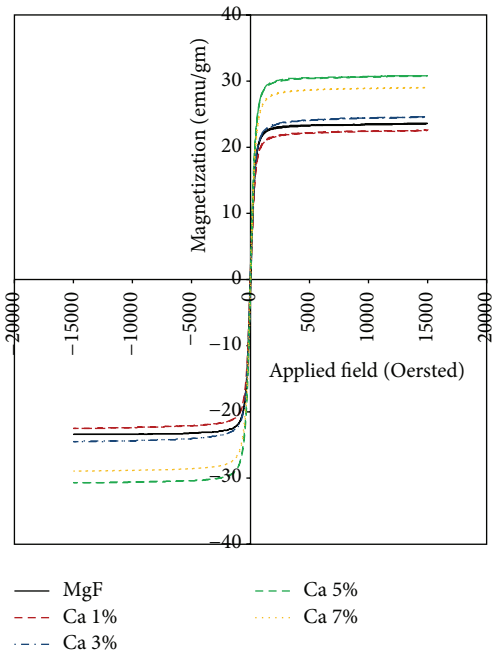

Figure 5: M-H curve showing variation of magnetization (emu/g) versus applied magnetic field (Oer) for pure and Ca substituted MgFe.

The measurement of bulk saturation magnetization can give the micromagnetic moment information, which can be related to the distribution of the magnetic ions in the interstitial sites [7].

According to Neel's theorem of sublattice [31, 32], the net magnetization will be

$$|M| = |M_B| - |M_A|. \quad (4)$$

The magnetization in each composition depends on the distribution of Fe^{3+} ions among the two sites A and B, where the Mg^{2+} and Ca^{2+} ions are nonmagnetic. As the magnesium ferrite is partly inverse in nature, so there is a probability of migration of a small fraction (y) of Mg^{2+} ions to A-sites [31]; in this case, the cation distribution can be represented as

$$\left(Mg_y^{2+}Fe_{1-y}^{3+}\right)^A\left[Mg_{1-y}^{2+}Fe_{1+y}^{3+}\right]^B O_4^{2-} \quad (5)$$

The first and the second bracket indicates tetrahedral (A-site) and octahedral (B-site) sublattice respectively. For $MgFe_2O_4$, the value of "y" is approximately equal to 0.1 [35]. The ionic magnetic moment of Mg^{2+} is zero (nonmagnetic) and the magnetic moment of Fe^{3+} is 5. The replacement of Fe^{3+} ion by "x" Ca^{2+} ions, where Ca^{2+} ions prefer to occupy A-site, gives $(1 - x - y)$ Fe^{3+} ions on the A-site and $(1 + x + y)$ Fe^{3+} ions on the B-site. This distribution will take the form:

$$\left(Ca_x^{2+}Mg_y^{2+}Fe_{1-x-y}^{3+}\right)^A\left[Mg_{1-x-y}^{2+}Fe_{1+x+y}^{3+}\right]^B O_4^{2-} \quad (6)$$

This substitution will lead to increasing Fe^{3+} ions on the B-site and consequently the magnetization of the B-site will increase and, at the same time, the magnetization of A-site will decrease according to the decrease of Fe^{3+} ion on A-site. Accordingly, the net magnetization will increase in the range $x \leq 0.05$ as given in the table. Further, the magnetization decreases with increasing "x" for $x > 0.05$. This behaviour may be related to the migration of Ca^{2+} ions to B-site, so that the cation distribution of formula (6) was applied to the range of $x \leq 0.05$, but, for $x > 0.05$, the cation distribution will be modified to the formula:

$$\left(Ca_{x-y}^{2+}Fe_{1+y-x}^{3+}\right)^A\left[Mg_{1-x}^{2+}Ca_y^{2+}Fe_{1+x-y}^{3+}\right]^B O_4^{2-} \quad (7)$$

From this distribution, the increase of calcium content will prevent the existence of Mg^{2+} ions on A-site. Also, the number of Fe^{3+} ions will decrease on B-site and increase on A-site by the same amount (i.e., y Fe^{3+} ions). This replacement will weaken the net magnetization of the whole lattice [32].

In case of Ca-ion distribution, it was reported [19, 27, 38] that Ca^{2+} ions strongly prefer to occupy the A-site for low Ca concentration; however, for high Ca concentration, Ca^{2+} ions either are distributed between A- and B-sites [10] or reside at the grain boundaries [20]. Carter and Mason [21] report that calcium at higher concentration segregates almost completely at the grain boundaries. Thus, according to the assumed cation distribution (Ca ions occupy the A-sites) increase of the Ca concentration from $x = 0.00$ to $x = 0.05$ leads Fe^{3+} content in B-site to increase and that in A-site to decrease. Hence, the total magnetization ($M = M_B - M_A$) increases. For $x > 0.05$, more Fe^{3+} ions migrate to B-site causing the B-B interaction to increase and hence the canting angle (θ_{yk}) is established. Therefore, it is suggested that significant canting exists at octahedral B-sites which can be explained on the basis of three-sublattice model suggested by Yafet and Kittel [39]. It is expected that (θ_{yk}) increases with increasing Ca concentration, such an increase in (θ_{yk}) leads to a decrease of M_s according to the equation $M_s = M_B \operatorname{Cos} \theta_{yk} - M_A$, where M_A and M_B are the magnetizations of A- and B-sites, respectively [40]. Thus, our results support the occupation of Ca ions for A-sites at low Ca concentration. Our observations also support the earlier work [41], where, for higher concentration of nonmagnetic ions, M_s decreases with "x" which is due to the weakening of A-B interaction and consequently stronger B-B interaction.

Figure 6 shows the magnetization versus temperature curves of pure and Ca^{2+} substituted Mg-ferrite for a field of 50 oersted. From this figure, the value of Curie temperature (T_C) (the temperature at which the value of magnetization reduces to zero) is calculated. The values of saturation magnetization, coercivity, retentivity, and Curie temperature are given in Table 4. It is clear from Table 4 that the value of Curie temperature decreases with increase in Ca^{2+} ions. The Curie temperature of a substituted ferrite will vary as per the variation in the relative strength of the A-B super exchange interactions due to nonmagnetic ion (Ca^{2+}) substitution in A-site. Since the present system has only one magnetic ion (Fe^{3+}), the variation of "T_C" is determined by the ratio of iron concentration in A and B sites in substituted ferrite with respect to that of an unsubstituted ferrite ($MgFe_2O_4$) [7]. The value of Curie temperature "T_C" for unsubstituted ferrite, that

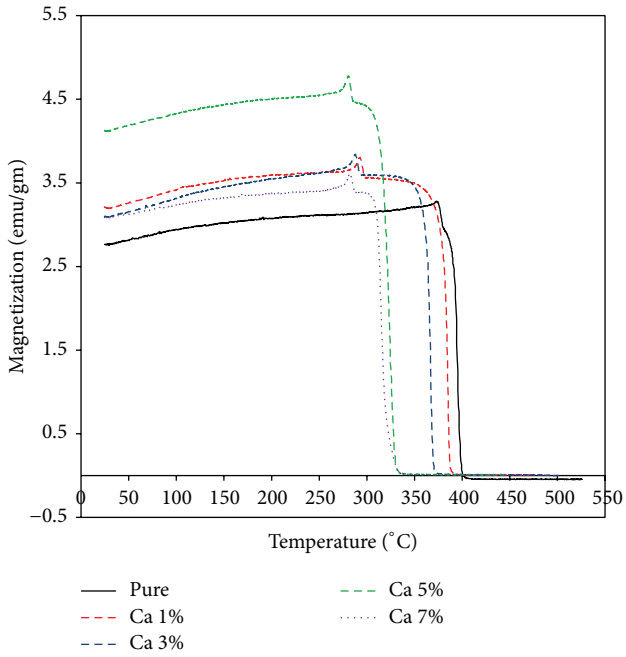

FIGURE 6: The saturation magnetization (M_S) as a function of temperature for pure and Ca substituted MgFe at a fixed field of 50 oersted.

is, $MgFe_2O_4$, is 400°C, which continuously decreases to 328°C for Ca 7% substituted Mg-ferrite. Initially, when the doping percentage is small ($x = 0.01$), very negligible Ca^{2+} ions go into the spinel and hence the number of magnetic ions on A-site is comparatively larger. Therefore, the A-B interaction is comparatively stronger resulting in slight decrease of curie temperature [20], whereas, with increased doping percentage from $x = 0.01$ to $x = 0.07$, the number of nonmagnetic ions (Ca^{2+}) occupying A-site reduces the magnetic moment of A-site [20], thereby making A-B interaction weaker which causes reduction in Curie temperature [20, 21, 28].

4. Conclusion

Structural and magnetic properties of magnesium ferrite (MgFe) and calcium substituted MgFe depend on several factors including method of preparation, chemical composition, and grain size of the particles. Pure and Ca substituted magnesium ferrite of the form $MgCa_xFe_{2-x}O_4$ (for $x = 0.00$, 0.01, 0.03, 0.05, 0.07) were successfully prepared by solid state reaction technique. The X-ray diffraction analysis confirms the formation of cubic spinel structure. The lattice parameter increases up to $x \leq 0.03$ and then starts decreasing for $x > 0.03$. The EDAX results confirm the presence of the required elements in the prepared composition. The magnetization increases for small Ca concentration, that is, $x \leq 0.05$, and then decreases for higher Ca concentration; that is, $x > 0.05$. The replacement of iron by calcium ions leads to cation distribution as explained in formula (6) and (7). $MgFe_2O_4$ represents the highest Curie temperature which decreases with the increase in substitution of nonmagnetic ion (Ca^{2+}). The presence of Mg^{2+} and Ca^{2+} ions on A-sites or on B-sites causes a decrease in Fe_A^{3+}-Fe_B^{3+} magnetic interaction, thereby lowering the Curie temperature.

Conflict of Interests

The authors declare that there is no conflict of interests regarding the publication of this paper.

References

[1] A. Pradeep, P. Priyadharsini, and G. Chandrasekaran, "Sol- gel route of synthesis of nanoparticles of $MgFe_2O_4$ and XRD, FTIR and VSM study," *Journal of Magnetism and Magnetic Materials*, vol. 320, no. 21, pp. 2774–2779, 2008.

[2] Ü. Özgür, Y. Alivov, and H. Morkoç, "Microwave ferrites, part 1: fundamental properties," *Journal of Materials Science: Materials in Electronics*, vol. 20, no. 9, pp. 789–834, 2009.

[3] W. V. Aulock, *Handbook of Microwaves Ferrites*, Materials Academic Press, New York, NY, USA, 1965.

[4] S. K. A. V Ahamed, K. Sahib, M. Suganthi, and C. Prakash, "Study of electrical and magnetic properties in nanosized Ce-Gd doped magnesium ferrite," *International Journal of Computer Applications*, vol. 27, no. 5, pp. 40–45, 2011.

[5] H. Knock and H. Dannheim, "Temperature dependence of the cation distribution in magnesium ferrite," *Physica Status Solidi (A)*, vol. 37, pp. K135–K137, 1976.

[6] E. De Grave, C. Dauwe, A. Govaert, and J. De Sitter, "Cation distribution and magnetic exchange interactions in $MgFe_2O_4$ studied by the mossbauer effect," *Physica Status Solidi (B) Basic Research*, vol. 73, no. 2, pp. 527–532, 1976.

[7] S. D. Chhaya, M. P. Pandya, M. C. Chhantbar, K. B. Modi, G. J. Baldha, and H. H. Joshi, "Study of substitution limit, structural, bulk magnetic and electrical properties of Ca^{2+} substituted magnesium ferrite," *Journal of Alloys and Compounds*, vol. 377, no. 1-2, pp. 155–161, 2004.

[8] M. Pavlovič, Č. Jovalekič, A. S. Nikolič, D. Manojlović, and N. Šojić, "Mechanochemical synthesis of stoichiometric $MgFe_2O_4$ spinel," *Journal of Materials Science: Materials in Electronics*, vol. 20, no. 8, pp. 782–787, 2009.

[9] H. H. Joshi and R. G. Kulkarni, "Susceptibility, magnetization and Mössbauer studies of the Mg-Zn ferrite system," *Journal of Materials Science*, vol. 21, no. 6, pp. 2138–2142, 1986.

[10] R. V. Upadhyay and R. G. Kulkarni, "The magnetic properties of the MgCd ferrite system by Mössbauer spectroscopy," *Materials Research Bulletin*, vol. 19, no. 5, pp. 655–661, 1984.

[11] R. A. Brand, H. Georges-Gibert, J. Hubsch, and J. A. Heller, "Ferrimagnetic to spin glass transition in the mixed spinel $Mg_{1+t}Fe_{2-2t}TitO_4$: a Mossbauer and DC susceptibility study," *Journal of Physics F: Metal Physics*, vol. 15, no. 9, pp. 1987–2007, 1985.

[12] K. B. Modi, H. H. Joshi, and R. G. Kulkarni, "Magnetic and electrical properties of Al^{3+}-substituted $MgFe_2O_4$," *Journal of Materials Science*, vol. 31, no. 5, pp. 1311–1317, 1996.

[13] G. J. Baldha, R. V. Upadhyay, and R. G. Kulkarni, "On the substitution of calcium in cobalt ferrite," *Journal of Materials Science*, vol. 23, no. 9, pp. 3357–3361, 1988.

[14] A. A. Sattar, H. M. El-Sayed, and W. R. Agami, "Physical and magnetic properties of calcium-substituted Li-Zn ferrite," *Journal of Materials Engineering and Performance*, vol. 16, no. 5, pp. 573–577, 2007.

[15] A. Y. Lipare, P. N. Vasambekar, and A. S. Vaingankar, "A.c. susceptibility study of $CaCl_2$ doped copper-zinc ferrite system," *Bulletin of Materials Science*, vol. 26, no. 5, pp. 493–497, 2003.

[16] C. Pasnicu, D. Condurache, and E. Luca, "Influence of substitution and addition of calcium on magnetic proprties of $Ni_{0.245}Zn_{0.755}Fe_2O_4$ ferrite," *Physica Status Solidi (A) Applied Research*, vol. 76, no. 1, pp. 145–150, 1983.

[17] C. Liu, B. Zou, A. J. Rondinone, and Z. J. Zhang, "Chemical control of superparamagnetic properties of magnesium and cobalt spinel ferrite nanoparticles through atomic level magnetic couplings," *Journal of the American Chemical Society*, vol. 122, no. 26, pp. 6263–6267, 2000.

[18] Q.-M. Wei, J.-B. Li, Y.-J. Chen, and Y.-S. Han, "X-ray study of cation distribution in $NiMn_{1-x}Fe_{2-x}O_4$ ferrites," *Materials Characterization*, vol. 47, no. 3-4, pp. 247–252, 2001.

[19] H. S. C. O'Neill and A. Navrotsky, "Cation distributions and thermodynamic properties of binary spinel solid solutions," *American Mineralogist*, vol. 69, no. 7-8, pp. 733–753, 1984.

[20] V. K. Singh, N. K. Khatri, and S. Lokanathan, "Mossbauer study of ferrite systems $Co_x\ Mn_{1-x}Fe_2O_4$ and $Ni_xMn_{1-x}Fe_2O_4$," *Pramana*, vol. 16, no. 4, pp. 273–280, 1981.

[21] D. C. Carter and T. O. Mason, "Electrical properties and site distribution of cations in $(Mn_yCo_{1-y})_{0.4}Fe_{2.6}O_4$," *Journal of the American Ceramic Society*, vol. 71, no. 4, pp. 213–218, 1988.

[22] E. D. Case, J. R. Smyth, and V. Monthei, "Grain size determinations," *Journal of the American Ceramic Society*, vol. 64, pp. C24–C25, 1981.

[23] C. Kittel, *Introduction a La Physique de L'etat Solide*, Dunod, Paris, France, 1958.

[24] W. B. Cross, L. Afflcck, M. V. Kuznetsov, I. P. Parkin, and Q. A. Pankhurst, "Self-propagating high-temperature synthesis of ferrites MFe_2O_4 (M = Mg, Ba, Co, Ni, Cu, Zn); reactions in an external magnetic field," *Journal of Materials Chemistry*, vol. 9, no. 10, pp. 2545–2552, 1999.

[25] C. G. Whinfrey, D. W. Eckart, and A. Tauber, "Preparation and X-ray diffraction data for some rare earth stannates," *Journal of the American Chemical Society*, vol. 82, no. 11, pp. 2695–2697, 1960.

[26] D. C. Khan, M. Misra, and A. R. Das, "Structure and magnetization studies of Ti-substituted $Ni_{0.3}\ Zn_{0.7}Fe_2O_4$," *Journal of Applied Physics*, vol. 53, no. 3, pp. 2722–2724, 1982.

[27] R. V. Upadhyay, G. J. Baldha, and R. G. Kulkarni, "Mössbauer study of the $Ca_xCo_{1-x}Fe_2O_4$ system," *Journal of Magnetism and Magnetic Materials*, vol. 61, no. 1-2, pp. 109–113, 1986.

[28] N. Rezlescu and E. Rezlescu, "Influence of additives on the material parameters of Li-Zn ferrites," *Physica Status Solidi (A) Applied Research*, vol. 147, no. 2, pp. 553–562, 1995.

[29] B. D. Cullity, *Elements of X-Ray Diffraction*, Addison-Wesley, Reading, Mass, USA, 2nd edition, 1978.

[30] A. A. Pandit, S. S. More, R. G. Dorik, and K. M. Jadhav, "Structural and magnetic properties of $Co_{1+y}Sn_yFe_{2-2y-x}Cr_xO_4$ ferrite system," *Bulletin of Materials Science*, vol. 26, no. 5, pp. 517–521, 2003.

[31] S. A. Mazen, S. F. Mansour, and H. M. Zaki, "Some physical and magnetic properties of Mg-Zn ferrite," *Crystal Research and Technology*, vol. 38, no. 6, pp. 471–478, 2003.

[32] K. J. Stanlley, *Oxide Magnetic Materials*, Clarendon Press, Oxford, UK, 1972.

[33] J. De Sitter, A. Govaert, E. De Grave, D. Chambaere, and G. Robbrecht, "Mossbauer study of Ca^{2+} containing magnetites," *Physica Status Solidi (A) Applied Research*, vol. 43, no. 2, pp. 619–624, 1977.

[34] E. De Grave, J. De Sitter, and R. Vandenberghe, "On the cation distribution in the spinel system yMg_2TiO_4-(1–y)$MgFe_2O_4$," *Applied Physics*, vol. 7, no. 1, pp. 77–80, 1975.

[35] J. Smit and H. P. J. Wijn, *Ferrites*, Cleaver-Hume Press, London, UK, 1959.

[36] T. F. W. Barth and E. Posnjak, "Spinel structures: with and without variate atom equipoints," *Zeitschrift für Kristallographie*, vol. 82, pp. 325–341, 1932.

[37] C. Guillaud, "Proprieties magnetiques des ferrites," *Journal de Physique et Le Radium*, vol. 12, pp. 239–248, 1951.

[38] N. Rezlescu and E. Rezlescu, "Effects of addition of Na_2O, Sb_2O_3, CaO, and ZrO_2 on the properties of lithium zinc ferrite," *Journal of the American Ceramic Society*, vol. 79, no. 8, pp. 2105–2108, 1996.

[39] Y. Yafet and C. Kittel, "Antiferromagnetic arrangements in ferrites," *Physical Review*, vol. 87, no. 2, pp. 290–294, 1952.

[40] S. S. Suryawanshi, V. V. Deshpande, U. B. Deshmukh, S. M. Kabur, N. D. Chaudhari, and S. R. Sawant, "XRD analysis and bulk magnetic properties of Al^{3+} substituted Cu-Cd ferrites," *Materials Chemistry and Physics*, vol. 59, no. 3, pp. 199–203, 1999.

[41] S. T. Alone and K. M. Jadhav, "Structural and magnetic properties of zinc-and aluminum-substituted cobalt ferrite prepared by co-precipitation method," *Pramana*, vol. 70, no. 1, pp. 173–181, 2008.